
Palm up: Playing in the Latent Manifold for Unsupervised Pretraining

Hao Liu*
UC Berkeley

Tom Zahavy
DeepMind

Volodymyr Mnih
DeepMind

Satinder Singh
DeepMind

Abstract

Large and diverse datasets have been the cornerstones of many impressive advancements in artificial intelligence. Intelligent creatures, however, learn by interacting with the environment, which changes the input sensory signals and the state of the environment. In this work, we aim to bring the best of both worlds and propose an algorithm that exhibits an exploratory behavior whilst it utilizes large diverse datasets. Our key idea is to leverage deep generative models that are pretrained on static datasets and introduce a dynamic model in the latent space. The transition dynamics simply mixes an action and a random sampled latent. It then applies an exponential moving average for temporal persistency, the resulting latent is decoded to image using pretrained generator. We then employ an unsupervised reinforcement learning algorithm to explore in this environment and perform unsupervised representation learning on the collected data. We further leverage the temporal information of this data to pair data points as a natural supervision for representation learning. Our experiments suggest that the learned representations can be successfully transferred to downstream tasks in both vision and reinforcement learning domains.

1 Introduction

Large and diverse datasets have been the cornerstones of many impressive successes at the frontier of artificial intelligence, such as protein folding [64, 28], image recognition [55, 13], and understanding natural language [6, 12]. Training machine learning models on diverse datasets that cover a breadth of human-written text and natural images often dramatically improves performance and enables impressive generalization capabilities [16, 6, 55, 12]. These models are learned from a fixed set of images, videos, or languages, guided by supervision that comes from ground-truth labels [13, 55], self-supervised contrastive learning [10], or masked token prediction [6, 12] among other approaches.

In contrast, intelligent creatures learn to perform interactions that actively change the input sensory signals and the state of the environment towards a desired configuration. For example, in psychology, it has been shown that interaction with the environment is vital for developing flexible and generalize intelligence [23, 74, 17]. During the first few months of interactions, infants develop meaningful understandings about objects [67] and prefer to look at exemplars from a novel class (e.g., dogs) after observing exemplars from a different class (e.g., cats) [54]. We hypothesize that by situating the agent in a high semantic complexity environment, the agent can develop interesting cognition abilities.

Given the effectiveness of learning from large and diverse datasets and the significance of interactive learning behaviors in intelligent creatures, it is therefore extremely important to connect them to build better learning algorithms.

To bridge the gap, perhaps one straightforward solution is learning in the diverse real world [1, 53], however, teaching a robot to interact in the physical world is both time consuming and resource

*This work was partially done at DeepMind. Correspondence to hao.liu@cs.berkeley.edu

intensive, and it is also difficult to scale up. An alternative is learning in simulated environments which have got surged interest recently. There simulators, such as Habitat [61, 70], RL Bench [27], House3D [77], and AI2THOR [36] enable the agent to interact with its environment. However, the visual complexity of these simulated environments is far from matching the intricate real world. The key limitation is that making hand-designed simulation that is close enough to what a camera in the real-world would capture is both challenging and tedious.

To remedy the issue, we propose a conceptually simple yet effective method that leverages existing diverse datasets, builds an environment with high semantic complexity from them, and then performs interactive learning in this environment. We do so by leveraging deep generative models that are trained in static datasets and introduce transition dynamics in the latent space of the generative model. Specifically, at each time step, the transition dynamics simply mix action and a random sampled latent. It then applies an exponential moving average for temporal persistency, imitating the prevalent temporal persistency in the real world. Finally, the resulting latent is decoded to an image using a trained generator. The generator is a conditional generative model which is conditioned on a prompt *e.g.* a class label sampled at the beginning of an episode for achieving further temporal persistency. For the generative model, we use conditional StyleGAN [32] in this work, chosen for its simplicity, although our method is not restricted to it, and can be also applied to other generative models such as language conditioned model Dalle [56].

We employ unsupervised reinforcement learning (RL) [41] to explore this environment motivated by imitating how intelligent creatures acquire perception and action skills by curiosity [23, 35, 60]. Specifically, we use the nonparametric entropy maximization method named APT [44] which encourages the agent to actively explore the environment to seek novel and unseen observations. Similar to other pixel-based unsupervised RL methods, APT learns an abstract representation by using off-the-shelf data augmentation and contrastive learning techniques from vision [37, 40, 39]. While effective, designing these techniques requires domain knowledge. We show that by simply leveraging the temporal nature, representation can be effectively learned. We do so by maximizing the similarity between representations of current and next observations based on siamese network [5] without needing to use domain knowledge or data augmentation. Our method is named as **playing** in the latent manifold for unsupervised pretraining (PALM).

We conduct experiments in CIFAR classification and out-of-distribution detection by transferring our unsupervised exploratory pretrained representations in StyleGAN-based environments. Our experiments show that the learned representations achieve competitive results with state-of-the-art methods in image recognition and out-of-distribution detection despite being only trained in synthesized data without data augmentation. We also train StyleGAN in observation data collected from Atari and apply our method to it. We found that the learned representation helped in maximizing many Atari game rewards. Our major contributions are summarized below:

- We present a surprisingly simple yet effective approach to leverage generative models as an interactive environment for unsupervised RL. By doing so, we connect vision datasets with RL, and enable learning representation by actively interacting with the environment.
- We demonstrate that exploration techniques used in unsupervised RL incentivize RL agent to learn representations from a synthetic environment without data augmentations.
- We show that PALM matches SOTA self-supervised representation learning methods on CIFAR and out-of-distribution benchmarks.
- We show that PALM outperforms strong model-free and model-based training from scratch RL. It also achieves competitive scores as SOTA exploratory pre-training RL and offline-data pretraining RL methods.

2 Related work

Exploratory pretraining in RL Having an unsupervised pretraining stage before finetuning on the target task has been explored in reinforcement learning to improve downstream task performance. One common approach has been to allow the agent a period of fully-unsupervised interaction with the environment, during which the agent is trained to maximize a surrogate exploration-based task such as the diversity of the states it encounters [44, 43, 78]. Others have proposed to use self-supervised objectives to generate intrinsic rewards encouraging agents to visit new states, such as the loss of an

inverse dynamics model [52, 7]. SGI [63] combines forward predictive representation learning [62] with inverse dynamics model [52] and demonstrate the power of representation pretraining for downstream RL tasks. Massive-scale unsupervised pretraining has shown strong results [8]. Laskin et al. [41] conducted a comparison of different unsupervised pretraining reinforcement learning algorithms. Finally, Chaplot et al. [9], Weihs et al. [75] studied training RL agent in game simulators and transferring its representation to various vision tasks. Their environments are equipped with carefully chosen domain-specific reward function to guide the learning of RL agent, and the architectures of their RL agents are fairly complicated.

Our work differs in that we do not rely on hand-crafted simulators and renderers which require a huge amount of domain knowledge and effort to build, instead we leverage generative models as renders. Unlike many prior work in unsupervised pretraining RL, our work does not focus on improving transfer performance to downstream RL tasks although it can be used for this purpose.

Training with synthetic data Using deep generative models as a source of synthetic data for representation learning has been studied in prior work [59, 26, 33]. These generative models are fit to real image datasets and produce realistic-looking images as samples. Baradad et al. [2] studied using data sampled from random initialized generative models to train contrastive representations. Goyal et al. [20] studied combining data sampled from pretrained generative models with real data for adversarial training and demonstrated improved results in robustness. The use of synthesized data has been explored in reinforcement learning under the heading of domain randomization [72], where 3D synthetic data is rendered under a variety of lighting conditions to transfer to real environments where the lighting may be unknown. Our approach does away with the hand crafted simulation engine entirely by making the training data diverse through unsupervised exploration.

Different from them, our work focus on leveraging a generative model as an interactive environment and learn representation without using data augmentation.

Temporal persistent representation Using temporal persistent information for representation learning has been proposed in the past with similar motivations as ours. It has been used in learning representation from videos [3, 76, 48, 19, 14, 51] by minimizing different metrics of representation difference over a temporal segment. Learning persistent representation has been explored in reinforcement learning, and has been demonstrated to improve data efficiency [50, 65, 62, 79] and improve downstream task performance [68, 63].

In relation to these prior efforts, our work studies visual representation learning from interacted experiences based on real-world data.

3 Preliminary

Unsupervised reinforcement learning Reinforcement learning considers the problem of finding an optimal policy for an agent that interacts with an uncertain environment and collects reward per action [69]. The agent maximizes its cumulative reward by interacting with its environment.

Formally, this problem can be viewed as a Markov decision process (MDP) defined by $(\mathcal{S}, \mathcal{A}, \mathcal{T}, \rho_0, r, \gamma)$ where $\mathcal{S} \subseteq \mathbb{R}^{n_s}$ is a set of n_s -dimensional states, $\mathcal{A} \subseteq \mathbb{R}^{n_a}$ is a set of n_a -dimensional actions, $\mathcal{T} : \mathcal{S} \times \mathcal{A} \times \mathcal{S} \rightarrow [0, 1]$ is the state transition probability distribution. $\rho_0 : \mathcal{S} \rightarrow [0, 1]$ is the distribution over initial states, $r : \mathcal{S} \times \mathcal{A} \rightarrow \mathbb{R}$ is the reward function, and $\gamma \in [0, 1)$ is the discount factor. At environment states $s \in \mathcal{S}$, the agent take actions $a \in \mathcal{A}$, in the (unknown) environment dynamics defined by the transition probability $T(s'|s, a)$, and the reward function yields a reward immediately following the action a_t performed in state s_t . In value-based reinforcement learning, the agent learns an estimate of the expected discounted return, a.k.a. state-action value function $Q^\pi(s_t, a_t) = \mathbb{E}_{s_{t+1}, a_{t+1}, \dots} [\sum_{l=0}^{\infty} \gamma^l r(s_{t+l}, a_{t+l})]$. A new policy can be derived from value function by acting ϵ -greedily with respect to the action values (discrete) or by using policy gradient to maximize the value function (continuous).

In unsupervised reinforcement learning, the reward function is defined as some form of intrinsic reward that is agnostic to standard task-specific reward function $r := r_{\text{intrinsic}}$. The intrinsic reward function is usually constructed for a better exploration and is computed using states and actions collected by the agent.

Generative adversarial model Generative Adversarial Networks (GANs) [18] consider the problem of generating photo realistic images. The StyleGAN [30, 32, 31] architecture is one of the state-of-the-art in high-resolution image generation for a multitude of different natural image categories such as faces, buildings, and animals.

To generate high-quality and high-resolution images, StyleGAN makes use of a specialized generator architecture which consists of a mapping network and synthesis network. The mapping network converts a latent vector $z \in \mathcal{Z}$ with $\mathcal{Z} \in \mathbb{R}^n$ into an intermediate latent space $w \in \mathcal{W}$ with $\mathcal{W} \in \mathbb{R}^n$. The mapping network is implemented using a multilayer perceptron that typically consists of 8 layers. The resulting vector w in that intermediate latent space is then transformed using learned affine transformations and used as an input to a synthesis network.

The synthesis network consists of multiple blocks that each takes three inputs. First, they take a feature map that contains the current content information of the image that is to be generated. Second, each block takes a transformed representation of the vector w as an input to its style parts, followed by a normalization of the feature map.

4 Method

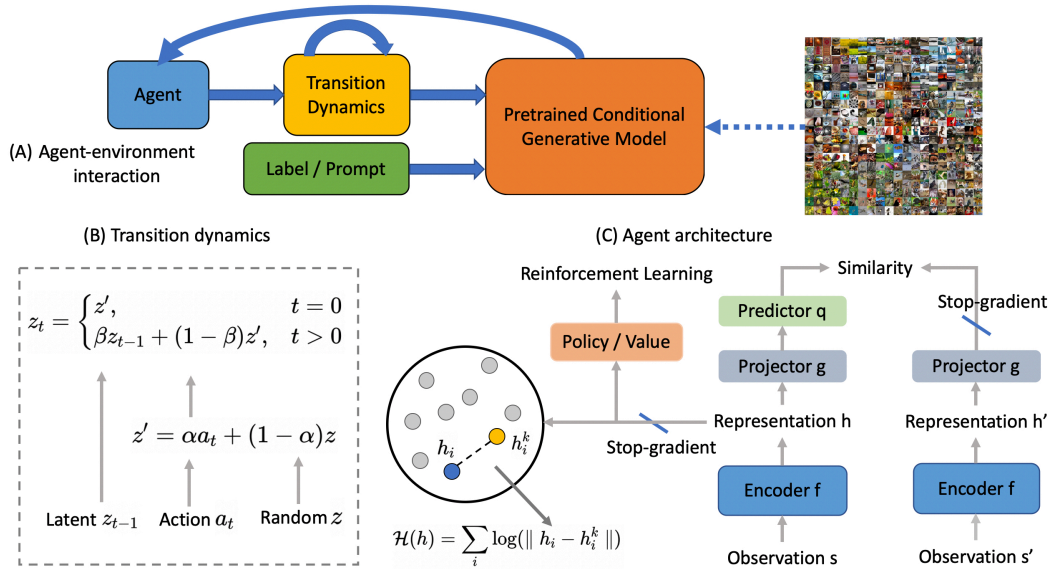


Figure 1: Overview of the proposed method. **(A)**. A conditional generative model is pretrained in a static dataset which is conditioned a prompt (*e.g.* language or class label) sampled at the beginning of an episode, and a transition dynamics is defined in the latent space of the generator, the agent maximizes the nonparametric entropy of experience in learned representation space. **(B)**. The transition dynamics consists of mixing a randomly sampled latent with action (of the same dimension) followed by exponential moving average for temporal persistency, the resulting latent is decoded to image using pretrained generator. **(C)**. The representation is learned without using data augmentation by maximizing the representation similarity between two consecutive synthesized observations based on Siamese network. The agent is updated using unsupervised reinforcement learning with representation detached.

Our objective is to leverage pretrained deep generative models $G : \mathcal{Z} \times \mathcal{C} \rightarrow \mathcal{S}$ where \mathcal{Z} denote latents, \mathcal{C} denote prompt or labels and \mathcal{S} denote observations to build an interactive environment and train an unsupervised reinforcement learning agent in such environment for representation pretraining.

4.1 Latent environment dynamics

The transition dynamics are designed in the latent space of StyleGAN. At the beginning of an episode, a class label or prompt c is randomly sampled, at each time step, c and a latent z_t that depends on the action and previous latent $z_t = T(a, z_{t-1})$ are transformed by the synthesis network of StyleGAN into an image which serves as an observation $s_t = G(z_t, c)$. We note that while the environment conditions on the label, the ground-truth information is not directly used by PALM.

The transition dynamics model consists of two steps. In the first step, it combines a randomly sampled latent z with the agent’s action to obtain a new latent $z' = T_{\text{com}}(z, a_t)$. Although more advanced combination methods can be used, we use simple weighted summation to combine latent and action $T_{\text{com}}(z, a_t) = \alpha a_t + (1 - \alpha)z$, where a is an action generated by the policy and $\alpha \in [0, 1]$ is a hyperparameter controls the relative importance of action and latent.

The second step is a transformation $T_{\text{ema}}(z')$ which is designed to ensure temporal persistency of the environment. We use a simple exponential moving average (EMA) to implement T_{ema} . Specifically, this module generate new latent by following

$$z_t = \begin{cases} z', & t = 0 \\ \beta z_{t-1} + (1 - \beta)z', & t > 0 \end{cases}$$

where z' is the combined latent and action, z_t is the exponential moving average at timestep t , and $\beta \in [0, 1]$ is a hyperparameter that controls how fast the environment changes in respond to agent. We used $\beta = 0.95$ in most of our experiments per our initial experiments.

The high β is motivated by observations in unsupervised RL and linguistics. It has been shown that a highly random environment hinders the learning of unsupervised RL agents which is also known as the "Noisy-TV" problem [7]. It also has an interesting connection to the uniform information density hypothesis in linguistics which states that—subject to the constraints of the grammar—humans prefer sentences that distribute information equally across the linguistic signal, *i.e.*, evenly distributed surprise [42].

In addition to the latent z_t , we also condition the generator $G(z, c)$ on a random sample class label c sampled at the beginning of an episode, resulting in further persistent consistency. Finally, the environment dynamics can be written as $T := \mathcal{G}(T_{\text{ema}}(T_{\text{com}}(z, a)), c)$.

4.2 Temporal persistent representation

Our goal is to pretrain a representation $f : \mathcal{S} \rightarrow \mathcal{H}$ which is a mapping that maps observations s to lower dimensional representations h , using the data (experience replay) collected by the agent. Data augmentations are key ingredients of unsupervised representation learning methods [see e.g. 10, 11]. However, designing augmentations requires domain knowledge.

Our representation learning is instead based on temporal information. Our key idea is that since each trajectory is generated by interacting with a deep generative model conditions on the same label and temporal persistent latent, it provides natural augmentations of visual content under various changing factors, such as occlusion and illumination. Some rollout trajectories during training are presented in Figure 2. In addition, the exploratory learning behavior of the agent increases the diversity of the trajectory.

Specifically, the idea is to train the encoder $f(s)$ to produce embeddings that are persistent in time in the same trajectory, *i.e.*, two presentations $h_t = f(s_t)$ and $h_{t+1} = f(s_{t+1})$ should be similar. To do so, we use the Siamese network [5] and its modern training techniques from SimSiam [11]. Specially, we maximize the similarity between $q(g(f(s)))$ and $\text{stop_gradient}(g(f(s')))$ where q and g are multilayer perceptrons. More details can be found in appendix.

4.3 Unsupervised exploration

The objective of unsupervised exploration is to maximize the diversity of the data seen by the agent, imitating how intelligent creatures develop recognition.

An observation s_t is first encoded using the encoder f to get representation $h_t = f(s_t)$. The policy takes representation h_t as input and generates action a_t of the same dimension. The policy distribution is a tanh Gaussian following prior work in unsupervised reinforcement learning [78, 41].

We resort to maximizing the nonparametric entropy of the representation space which has been widely used in unsupervised reinforcement learning [66, 4, 44, 78]. By explicitly encouraging the agents to visit diverse states, it effectively encourages the agents to explore environments, and thus learn more diverse behaviors. The estimator computes the distance between each particle $h_i = f(s_i)$ and its k -th

nearest neighbor h_i^* .

$$H(h) = \sum p(h) \log p(h) \propto \sum_{i=1}^n \log \|h_i - h_i^*\|_2,$$

where $\|\cdot\|_2$ is ℓ_2 norm. We associate each transition from experience replay $\{(s, a, s')\}$ with an intrinsic reward given by

$$r_{\text{intrinsic}}(s, a, s') = \log \|h - h_i^*\|_2.$$

Putting everything together, the diagram of our method is shown in Figure 1.

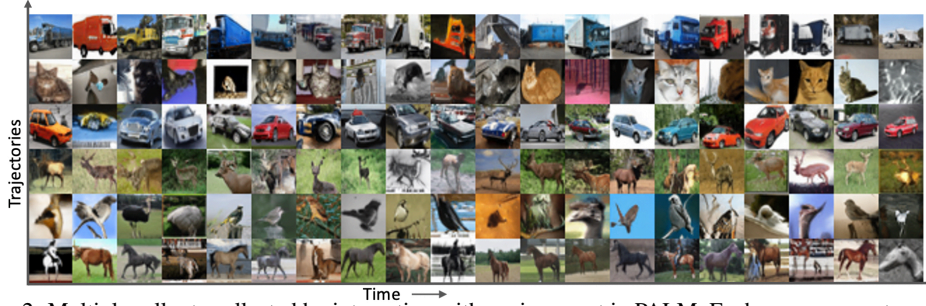


Figure 2: Multiple rollouts collected by interacting with environment in PALM. Each row represents a randomly sampled segment of a trajectory. From top to bottom, each trajectory is conditioned on a different class label c .

5 Results

It is important to stress that this work focuses on studying how combined exploratory pretraining and static datasets contribute to representation learning in artificial agents and not on developing a new, state-of-the-art, methodology for representation learning. Nevertheless, to better situate our results in the context of existing work, we provide strong baselines in our experiments.

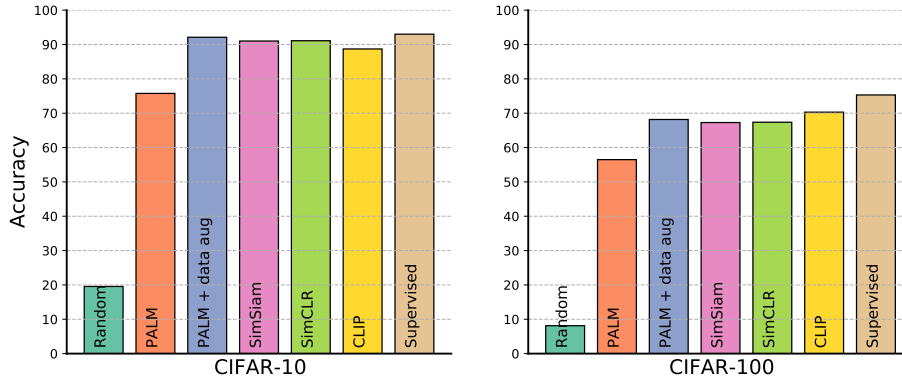


Figure 3: Linear classification results from different methods in CIFAR datasets. Model is ResNet-18 except for CLIP [55] which is based on ResNet-50. Supervised ResNet [22] is trained from scratch. SimCLR [10] and SimSiam [11] are pretrained on CIFAR dataset. CLIP [55] is pretrained on paired image-text datasets. We use reported scores of each baseline for comparison. All results of our method are the average of three runs with different seeds. PALM (our method) actively collect synthesized data from deep generative models based environment. The representation is learned without using data augmentation from explored experience but still achieves competitive results. Our PALM, which is based on SimSiam [11], is compatible with data augmentation, by adding the same data augmentation used in SimSiam, PALM + data aug matches or outperforms state-of-the-art static representation learning algorithms.

Image classification We test PALM on image classification tasks using a ResNet-18 as encoder f . The RL agent interacts with the environment for 50M steps, and trains representation using the procedure described in the method section. The hyperparameters of the representation learning follow the default hyperparameters of SimSiam [11] and more details can be found in the supplemental material.

We compare our method with a series of strong methods in static datasets, including state-of-the-art contrastive representation learning methods SimCLR [10] and SimSiam, supervised trained model, and CLIP [55] which is pretrained on a large-scale paired image-text datasets.

Figure 3 shows the linear classification performance of each method, PALM is surprisingly effective given the lack of data augmentation and real data. Note that the baselines do not have an option not to use data augmentation.

Additionally, adding the same data augmentation techniques used in SimSiam to our method further improves the results, matching or outperforming current SOTA static representation learning algorithms. Compared with the SOTA method SimSiam, PALM + data augmentation actively explore an environment instead of using a static dataset, and the representation learning and data augmentation are applied to synthesized temporal pair instead of two views of the same image.

Table 1: AUROC (%) of classifiers trained on CIFAR-10. Models are ResNet-18. The reported results of PALM are averaged over five trials. To have a rigorous comparison, the results of baselines are from their papers. A \rightarrow B denotes in-distribution dataset A and out-of-distribution dataset B. Subscripts denote standard deviation, and bold denote the best results.

Train method	CIFAR10 \rightarrow				
	SVHN	LSUN	CIFAR100	Interp.	CelebA
Standard [24]	88.6 \pm 0.9	90.7 \pm 0.5	85.8 \pm 0.3	75.4 \pm 0.7	64.1 \pm 0.5
SupCLR [34]	97.3 \pm 0.1	92.8 \pm 0.5	88.6 \pm 0.2	75.7 \pm 0.1	73.2 \pm 0.3
CSI [71]	96.5 \pm 0.2	96.3\pm0.5	90.5 \pm 0.1	78.5 \pm 0.2	75.1 \pm 0.3
PALM (ours)	97.9\pm0.2	96.1 \pm 0.3	91.5\pm0.2	79.9\pm0.2	76.8\pm0.4

Out-of-distribution detection While some prior work demonstrated that self-supervised learning approaches significantly improve OOD detection performance [25, 15], their self-supervised pre-train heavily relies on domain-specific data augmentations, we want to study how PALM performs on OOD benchmarks.

We compare PALM with standard supervised model [22, 24] and contrastive representation learning based methods including SupCLR [34] and CSI [71]. CSI demonstrates state-of-the-art results by combining contrastive representation learning and supervised learning. Table 1 shows the comparison on multiple datasets. PALM outperforms CSI in 4 out of 5 out-of-the-distribution datasets, despite using only synthesized data and no data augmentation. We attribute the effectiveness of PALM on OOD detection to active exploration stimulates the model to learn the invariance of data. In doing so, the representation is optimized for distinguishing different observations.

Data efficient representation in RL In this experiment, we are interested in testing PALM pre-trained model for downstream reinforcement learning tasks. To do so, we focus our experimentation on the Atari 100k benchmark introduced by Kaiser et al. [29], in which agents are allowed only 100k steps of interaction with their environment. There has been extensive usage of Atari for representation learning and exploratory pretraining [8, 44, 63, 21]. Finetuning after exploratory pretraining is highly effective [e.g., 63, 8], providing strong baselines to compare to.

Unlike experiments in CIFAR datasets, here we train an unconditional StyleGAN model in a dataset collected by running a double DQN [47, 73] agent. The dataset consists of 50M frames for each game. We use 6M steps for exploratory pretraining in the synthesized environment and we utilize DrQ [37] for online finetuning. Table 2 shows the comparison of PALM with baselines. Comparing

Table 2: HNS on Atari100k for PALM and baselines. >H denotes super-human performance and >0 denotes greater than random performance. Mdn and mean denote the median and mean scores. Bold denote the best results in each category.

Method	Mdn	Mn	>H	>0	Data
<i>No Pretraining (Finetuning Only)</i>					
SimPLe	0.144	0.443	2	26	0
DrQ	0.268	0.357	2	24	0
<i>Exploratory Pretraining + Finetuning</i>					
APT	0.475	0.666	7	26	250M
ATC	0.237	0.462	3	26	3M
SGI	0.456	0.838	6	26	6M
<i>Offline-data Pretraining + Finetuning</i>					
ATC	0.219	0.587	4	26	3M
SGI	0.753	1.598	9	26	6M
<i>Synthesized Exploratory Pretraining + Finetuning</i>					
PALM (ours)	0.298	0.411	2	26	50M + 6M

with exploratory pretraining baselines (APT [44], ATC [68], and SGI [63]) that are pretrained in Atari games directly, PALM achieves surprisingly good results considering that it is trained in a simple synthesized environment. PALM achieves higher medium and mean score than DrQ in Atari 100k despite the online finetuning of PALM is the same as DrQ, demonstrating the benefit of pretrained representation. Compared with offline-data pretraining baselines (ATC and SGI), there is still a gap between PALM and the state-of-the-arts, which is probably due to PALM’s environment being trained on observations only while ATC and SGI are trained on both observations and actions in a model-based style. Worth mentioning that while PALM utilizes 50M offline action-free experience for pretraining, the amount is less than the 250M online action labeled experience used in APT. We would like to emphasize that DrQ is based on data augmentation, but PALM can outperform DrQ without data augmentation given the same amount of online experience.

6 Analysis

Persistent environment and active interaction are important.

Next, we perform an ablation study, to study the importance of a persistent environment. We aim to answer the following question. How important it is to have action (controlled by α) and state (controlled by β) in the transition dynamics? When $\beta = 0$, there is effectively no state, *i.e.*, its a bandit. As shown in Figure 4, when decreasing the importance of states which is denoted as PALM ($\alpha = 0.5 \beta = 0.5$), the performance decreases. The extreme case $\beta = 0$ shows a significant drop in accuracy. These results indicate that it is important to have temporal persistent transition dynamics. When $\alpha = 0$, action is ignored in transition dynamics, this ablative baseline performs significantly worse than its default $\alpha = 0.5$. When replacing the agent’s action with random noise which is denoted as PALM + random action, we also see a significant performance drop. These results show having active interaction is important to the results of PALM. We present the results of more combinations of α and β in Figure 5, the results show that as α decreases from 0.95 to 0, because of the decreasing importance of action, the accuracy continues to drop. $\alpha = 0.95$ in general performs better than $\alpha = 1.0$, indicates mixing a small amount of random noise with action helps exploration and improves representation learning. When α or β is zero, the results are significantly worse. We also see that $\beta \in [0.5, 0.75]$ performs significantly better than other values, showing that persistence of dynamics is crucial.

Exploratory Learning as Curriculum Learning.

As we have seen, representations learned from exploratory learning in a synthesized environment can be surprisingly powerful. We are interested in having a perhaps preliminary study of the reasons.

To do so, we compare PALM with its passive version (passive PALM), static version (static PALM), and methods proposed in Jahanian et al. [26]. In the random variant, the positives pairs are sampled from $G(z, c = c')$ (*i.e.* fix the class, take two random draws from z). We denote this baseline as Random Jahanian et al. In Gaussian Jahanian et al, the positive pairs are given by z and $z+w$, where w is Gaussian.

Static PALM is not trained in the interactive environment, instead, it is trained with real images. Specifically, we randomly sample two images of the same label from a dataset and use them as a temporal pair to train the representation learning of PALM. We note that static PALM is related to SupCon [34], but it differs in that static PALM does not use any data augmentation while SupCon leverages a

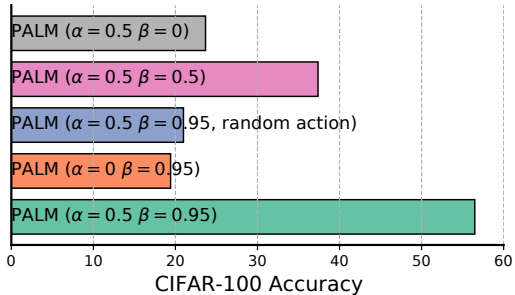


Figure 4: Ablative analysis of PALM on CIFAR-100 dataset. All results are the average of three runs with different seeds.

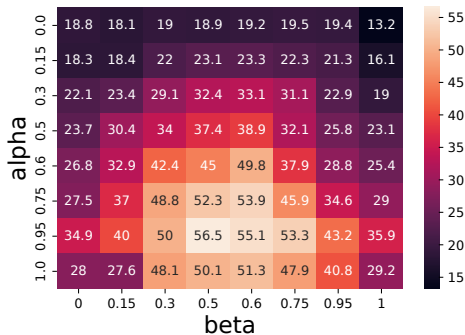


Figure 5: Ablative analysis of PALM on CIFAR-100 dataset. All results are the average of three runs with different seeds.

combination of data augmentations. SupCon also uses a large number of negative examples from different categories.

Passive PALM is trained offline on the experience of PALM. We first store all the online experience (50M in total) of PALM, then we use the saved experience to train passive PALM without having to interact with the environment. We consider two options of passive PALM. The first one is random passive PALM which randomly samples consecutive observations from the stored offline experience. The second one is ordered passive PALM which is trained on the same order of observations as in online experience.

With the number of data increasing, PALM keeps improving with the amount of training data and significantly outperforms static PALM even though static PALM is trained on real datasets. We believe the reason is that the diverse synthesized data collected by PALM can greatly help to learn representation. In the low data regime, carefully designed non-active learning based methods [26] outperforms PALM, possibly due to RL training being sample inefficient. With the increasing number of synthesized samples, PALM continues to improve and significantly outperform all baselines. The results also show that PALM scales better than non active learning based methods. PALM nearly always outperforms random passive PALM, demonstrating the effectiveness of exploratory learning. Interestingly but not surprisingly, ordered passive PALM performs nearly the same as PALM, indicating the exploratory learning behavior of PALM might play an important role in curriculum learning. The agent is optimized to search for novel samples in terms of their representation, by doing so, the searched samples should become more difficult to distinguish. We believe a comprehensive understanding of the effectiveness of PALM is out of the scope of this work, we tend to leave it as future work.

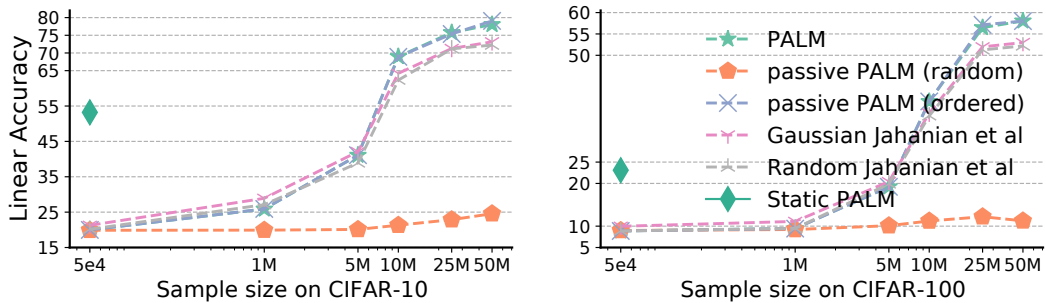


Figure 6: Results of comparing static and passive variants of the proposed method on CIFAR dataset. Sample size denotes the number of images for static PALM and denotes the number of interactions for others. All results are the average of three runs with different seeds.

Diversity analysis. In order to measure the diversity of the sampled synthetic data, we randomly sample 10K images from the CIFAR-10 train set and generate 10K images from StyleGAN by random sample latents. We also generate 10K images with PALM in latent space. For each sample in each set, we find its closest neighbor in Inception feature space (obtained after the pooling layer). The coverage is defined as the proportion of nearest neighbors that are unique in the train set. A better active exploration method would produce samples that are equally likely to be close to any image in the train set. PALM achieves a better coverage score than random sampling in latent space. Although the Euclidean distance in Inception feature space is inaccurate, the better coverage achieved by PALM indicates that by exploring the latent manifold it gets more diverse data.

Table 3: Analysis of diversity of generated data points on CIFAR-100.

Method	Coverage (%) (higher is better)
Latent space uniform sample	50.16
PALM	58.87

7 Conclusion and discussion

Our work presents a method to connect learning from large, diverse static datasets and learning by interaction, and demonstrates promising results of doing so. We believe it opens up an interesting future direction for advancing both reinforcement learning and self-supervised visual representation learning.

For limitations, since it is computational expensive to draw samples from large generative model, interacting with such environment is significantly slower than well optimized physical simulations used in RL, *e.g.*, Mujoco. Addressing such limitation would make this work more accessible and facilitate future research.

For future work, it would be interesting to design or learn better transition dynamics. It would be also interesting to evaluate our method in RL settings where a lot of action-free data are available and won't have to be collected (Minecraft for example). It would be also interesting to use a language conditioned generative model as an alternative *e.g.* Dalle [57, 58], so the environment has more complexity by prompting it with natural language.

Acknowledgements

We would like to thank Guillaume Desjardins for insightful discussion and giving constructive comments. We would also like to thank anonymous reviewers for their helpful feedback.

References

- [1] P. Agrawal, A. Nair, P. Abbeel, J. Malik, and S. Levine. Learning to poke by poking: Experiential learning of intuitive physics. In *Advances in Neural Information Processing Systems 29: Annual Conference on Neural Information Processing Systems 2016, December 5-10, 2016, Barcelona, Spain, 2016*.
- [2] M. Baradad, J. Wulff, T. Wang, P. Isola, and A. Torralba. Learning to see by looking at noise. *arXiv preprint arXiv:2106.05963*, 2021.
- [3] S. Becker. Learning temporally persistent hierarchical representations. In *Advances in neural information processing systems*, pages 824–830. Citeseer, 1997.
- [4] J. Beirlant. Nonparametric entropy estimation: An overview. *International Journal of the Mathematical Statistics Sciences*, 6:17–39, 1997.
- [5] J. Bromley, J. W. Bentz, L. Bottou, I. Guyon, Y. LeCun, C. Moore, E. Säckinger, and R. Shah. Signature verification using a “siamese” time delay neural network. *International Journal of Pattern Recognition and Artificial Intelligence*, 7(04):669–688, 1993.
- [6] T. B. Brown, B. Mann, N. Ryder, M. Subbiah, J. Kaplan, P. Dhariwal, A. Neelakantan, P. Shyam, G. Sastry, A. Askell, S. Agarwal, A. Herbert-Voss, G. Krueger, T. Henighan, R. Child, A. Ramesh, D. M. Ziegler, J. Wu, C. Winter, C. Hesse, M. Chen, E. Sigler, M. Litwin, S. Gray, B. Chess, J. Clark, C. Berner, S. McCandlish, A. Radford, I. Sutskever, and D. Amodei. Language models are few-shot learners. In *Advances in Neural Information Processing Systems 33: Annual Conference on Neural Information Processing Systems 2020, NeurIPS 2020, December 6-12, 2020, virtual, 2020*.
- [7] Y. Burda, H. Edwards, D. Pathak, A. J. Storkey, T. Darrell, and A. A. Efros. Large-scale study of curiosity-driven learning. In *7th International Conference on Learning Representations, ICLR 2019, New Orleans, LA, USA, May 6-9, 2019*. OpenReview.net, 2019.
- [8] V. Campos, P. Sprechmann, S. S. Hansen, A. Barreto, C. Blundell, A. Vitvitskyi, S. Kapturowski, and A. P. Badia. Coverage as a principle for discovering transferable behavior in reinforcement learning, 2021.
- [9] D. S. Chaplot, M. Dalal, S. Gupta, J. Malik, and R. R. Salakhutdinov. Seal: Self-supervised embodied active learning using exploration and 3d consistency. *Advances in Neural Information Processing Systems*, 34, 2021.
- [10] T. Chen, S. Kornblith, M. Norouzi, and G. E. Hinton. A simple framework for contrastive learning of visual representations. In *Proceedings of the 37th International Conference on Machine Learning, ICML 2020, 13-18 July 2020, Virtual Event*, volume 119 of *Proceedings of Machine Learning Research*, pages 1597–1607. PMLR, 2020.
- [11] X. Chen and K. He. Exploring simple siamese representation learning. In *Proceedings of the IEEE/CVF Conference on Computer Vision and Pattern Recognition*, pages 15750–15758, 2021.

- [12] J. Devlin, M.-W. Chang, K. Lee, and K. Toutanova. BERT: Pre-training of deep bidirectional transformers for language understanding. In *Proceedings of the 2019 Conference of the North American Chapter of the Association for Computational Linguistics: Human Language Technologies, Volume 1 (Long and Short Papers)*, pages 4171–4186, Minneapolis, Minnesota, 2019. Association for Computational Linguistics. doi: 10.18653/v1/N19-1423.
- [13] A. Dosovitskiy, L. Beyer, A. Kolesnikov, D. Weissenborn, X. Zhai, T. Unterthiner, M. Dehghani, M. Minderer, G. Heigold, S. Gelly, et al. An image is worth 16x16 words: Transformers for image recognition at scale. *arXiv preprint arXiv:2010.11929*, 2020.
- [14] C. Feichtenhofer, H. Fan, B. Xiong, R. Girshick, and K. He. A large-scale study on unsupervised spatiotemporal representation learning. In *Proceedings of the IEEE/CVF Conference on Computer Vision and Pattern Recognition*, pages 3299–3309, 2021.
- [15] S. Fort, J. Ren, and B. Lakshminarayanan. Exploring the limits of out-of-distribution detection. *Advances in Neural Information Processing Systems*, 34, 2021.
- [16] R. Geirhos, K. Narayanappa, B. Mitzkus, T. Thieringer, M. Bethge, F. A. Wichmann, and W. Brendel. Partial success in closing the gap between human and machine vision. *arXiv preprint arXiv:2106.07411*, 2021.
- [17] J. J. Gibson. *The ecological approach to visual perception: classic edition*. Psychology Press, 2014.
- [18] I. J. Goodfellow, J. Pouget-Abadie, M. Mirza, B. Xu, D. Warde-Farley, S. Ozair, A. C. Courville, and Y. Bengio. Generative adversarial nets. In *Advances in Neural Information Processing Systems 27: Annual Conference on Neural Information Processing Systems 2014, December 8-13 2014, Montreal, Quebec, Canada*, pages 2672–2680, 2014.
- [19] R. Goroshin, J. Bruna, J. Tompson, D. Eigen, and Y. LeCun. Unsupervised learning of spatiotemporally coherent metrics. In *Proceedings of the IEEE international conference on computer vision*, pages 4086–4093, 2015.
- [20] S. Gowal, S.-A. Rebuffi, O. Wiles, F. Stimberg, D. A. Calian, and T. A. Mann. Improving robustness using generated data. *Advances in Neural Information Processing Systems*, 34, 2021.
- [21] S. Hansen, W. Dabney, A. Barreto, D. Warde-Farley, T. V. de Wiele, and V. Mnih. Fast task inference with variational intrinsic successor features. In *8th International Conference on Learning Representations, ICLR 2020, Addis Ababa, Ethiopia, April 26-30, 2020*. OpenReview.net, 2020.
- [22] K. He, X. Zhang, S. Ren, and J. Sun. Deep residual learning for image recognition. In *2016 IEEE Conference on Computer Vision and Pattern Recognition, CVPR 2016, Las Vegas, NV, USA, June 27-30, 2016*, pages 770–778. IEEE Computer Society, 2016. doi: 10.1109/CVPR.2016.90.
- [23] R. Held and A. Hein. Movement-produced stimulation in the development of visually guided behavior. *Journal of comparative and physiological psychology*, 56(5):872, 1963.
- [24] D. Hendrycks and K. Gimpel. A baseline for detecting misclassified and out-of-distribution examples in neural networks. In *5th International Conference on Learning Representations, ICLR 2017, Toulon, France, April 24-26, 2017, Conference Track Proceedings*. OpenReview.net, 2017.
- [25] D. Hendrycks, K. Lee, and M. Mazeika. Using pre-training can improve model robustness and uncertainty. In *Proceedings of the 36th International Conference on Machine Learning, ICML 2019, 9-15 June 2019, Long Beach, California, USA*, volume 97 of *Proceedings of Machine Learning Research*, pages 2712–2721. PMLR, 2019.
- [26] A. Jahanian, X. Puig, Y. Tian, and P. Isola. Generative models as a data source for multiview representation learning. *arXiv preprint arXiv:2106.05258*, 2021.
- [27] S. James, Z. Ma, D. R. Arrojo, and A. J. Davison. Rlbench: The robot learning benchmark & learning environment. *IEEE Robotics and Automation Letters*, 5(2):3019–3026, 2020.
- [28] J. Jumper, R. Evans, A. Pritzel, T. Green, M. Figurnov, O. Ronneberger, K. Tunyasuvunakool, R. Bates, A. Židek, A. Potapenko, et al. Highly accurate protein structure prediction with alphafold. *Nature*, 596(7873):583–589, 2021.
- [29] L. Kaiser, M. Babaeizadeh, P. Milos, B. Osinski, R. H. Campbell, K. Czechowski, D. Erhan, C. Finn, P. Kozakowski, S. Levine, A. Mohiuddin, R. Sepassi, G. Tucker, and H. Michalewski. Model based reinforcement learning for atari. In *8th International Conference on Learning Representations, ICLR 2020, Addis Ababa, Ethiopia, April 26-30, 2020*. OpenReview.net, 2020.

- [30] T. Karras, S. Laine, and T. Aila. A style-based generator architecture for generative adversarial networks. In *Proceedings of the IEEE/CVF Conference on Computer Vision and Pattern Recognition*, pages 4401–4410, 2019.
- [31] T. Karras, M. Aittala, J. Hellsten, S. Laine, J. Lehtinen, and T. Aila. Training generative adversarial networks with limited data. *arXiv preprint arXiv:2006.06676*, 2020.
- [32] T. Karras, S. Laine, M. Aittala, J. Hellsten, J. Lehtinen, and T. Aila. Analyzing and improving the image quality of stylegan. In *Proceedings of the IEEE/CVF Conference on Computer Vision and Pattern Recognition*, pages 8110–8119, 2020.
- [33] H. Kataoka, K. Okayasu, A. Matsumoto, E. Yamagata, R. Yamada, N. Inoue, A. Nakamura, and Y. Satoh. Pre-training without natural images. In *Proceedings of the Asian Conference on Computer Vision*, 2020.
- [34] P. Khosla, P. Teterwak, C. Wang, A. Sarna, Y. Tian, P. Isola, A. Maschinot, C. Liu, and D. Krishnan. Supervised contrastive learning. In *Advances in Neural Information Processing Systems 33: Annual Conference on Neural Information Processing Systems 2020, NeurIPS 2020, December 6-12, 2020, virtual*, 2020.
- [35] C. Kidd and B. Y. Hayden. The psychology and neuroscience of curiosity. *Neuron*, 88(3): 449–460, 2015.
- [36] E. Kolve, R. Mottaghi, W. Han, E. VanderBilt, L. Weihs, A. Herrasti, D. Gordon, Y. Zhu, A. Gupta, and A. Farhadi. Ai2-thor: An interactive 3d environment for visual ai. *arXiv preprint arXiv:1712.05474*, 2017.
- [37] I. Kostrikov, D. Yarats, and R. Fergus. Image augmentation is all you need: Regularizing deep reinforcement learning from pixels. *arXiv preprint arXiv:2004.13649*, 2020.
- [38] A. Krizhevsky et al. Learning multiple layers of features from tiny images. 2009.
- [39] M. Laskin, K. Lee, A. Stooke, L. Pinto, P. Abbeel, and A. Srinivas. Reinforcement learning with augmented data. *arXiv:2004.14990*, 2020.
- [40] M. Laskin, A. Srinivas, and P. Abbeel. CURL: contrastive unsupervised representations for reinforcement learning. In *Proceedings of the 37th International Conference on Machine Learning, ICML 2020, 13-18 July 2020, Virtual Event*, volume 119 of *Proceedings of Machine Learning Research*, pages 5639–5650. PMLR, 2020.
- [41] M. Laskin, D. Yarats, H. Liu, K. Lee, A. Zhan, K. Lu, C. Cang, L. Pinto, and P. Abbeel. Urlb: Unsupervised reinforcement learning benchmark. *arXiv preprint arXiv:2110.15191*, 2021.
- [42] R. Levy and T. F. Jaeger. Speakers optimize information density through syntactic reduction. *Advances in neural information processing systems*, 19:849, 2007.
- [43] H. Liu and P. Abbeel. Aps: Active pretraining with successor features. In *International Conference on Machine Learning*, pages 6736–6747. PMLR, 2021.
- [44] H. Liu and P. Abbeel. Behavior from the void: Unsupervised active pre-training. *arXiv preprint arXiv:2103.04551*, 2021.
- [45] Z. Liu, P. Luo, X. Wang, and X. Tang. Deep learning face attributes in the wild. In *2015 IEEE International Conference on Computer Vision, ICCV 2015, Santiago, Chile, December 7-13, 2015*, pages 3730–3738. IEEE Computer Society, 2015. doi: 10.1109/ICCV.2015.425.
- [46] I. Loshchilov and F. Hutter. Sgdr: Stochastic gradient descent with warm restarts. *arXiv preprint arXiv:1608.03983*, 2016.
- [47] V. Mnih, K. Kavukcuoglu, D. Silver, A. A. Rusu, J. Veness, M. G. Bellemare, A. Graves, M. Riedmiller, A. K. Fidjeland, G. Ostrovski, et al. Human-level control through deep reinforcement learning. *nature*, 518(7540):529–533, 2015.
- [48] H. Mobahi, R. Collobert, and J. Weston. Deep learning from temporal coherence in video. In *Proceedings of the 26th Annual International Conference on Machine Learning*, pages 737–744, 2009.
- [49] Y. Netzer, T. Wang, A. Coates, A. Bissacco, B. Wu, and A. Y. Ng. Reading digits in natural images with unsupervised feature learning. 2011.
- [50] A. v. d. Oord, Y. Li, and O. Vinyals. Representation learning with contrastive predictive coding. *arXiv preprint arXiv:1807.03748*, 2018.

- [51] A. E. Orhan, V. V. Gupta, and B. M. Lake. Self-supervised learning through the eyes of a child. *arXiv preprint arXiv:2007.16189*, 2020.
- [52] D. Pathak, P. Agrawal, A. A. Efros, and T. Darrell. Curiosity-driven exploration by self-supervised prediction. In *Proceedings of the 34th International Conference on Machine Learning, ICML 2017, Sydney, NSW, Australia, 6-11 August 2017*, volume 70 of *Proceedings of Machine Learning Research*, pages 2778–2787. PMLR, 2017.
- [53] L. Pinto and A. Gupta. Supersizing self-supervision: Learning to grasp from 50k tries and 700 robot hours. In *2016 IEEE international conference on robotics and automation (ICRA)*, pages 3406–3413. IEEE, 2016.
- [54] P. C. Quinn, P. D. Eimas, and S. L. Rosenkrantz. Evidence for representations of perceptually similar natural categories by 3-month-old and 4-month-old infants. *Perception*, 22(4):463–475, 1993.
- [55] A. Radford, J. W. Kim, C. Hallacy, A. Ramesh, G. Goh, S. Agarwal, G. Sastry, A. Askell, P. Mishkin, J. Clark, G. Krueger, and I. Sutskever. Learning transferable visual models from natural language supervision. In *International Conference on Machine Learning (ICML)*, volume 139, pages 8748–8763, 2021.
- [56] A. Ramesh, M. Pavlov, G. Goh, S. Gray, C. Voss, A. Radford, M. Chen, and I. Sutskever. Zero-shot text-to-image generation. *arXiv preprint arXiv:2102.12092*, 2021.
- [57] A. Ramesh, M. Pavlov, G. Goh, S. Gray, C. Voss, A. Radford, M. Chen, and I. Sutskever. Zero-shot text-to-image generation. *arXiv preprint arXiv: Arxiv-2102.12092*, 2021.
- [58] A. Ramesh, P. Dhariwal, A. Nichol, C. Chu, and M. Chen. Hierarchical text-conditional image generation with clip latents. *arXiv preprint arXiv: Arxiv-2204.06125*, 2022.
- [59] S. Ravuri and O. Vinyals. Classification accuracy score for conditional generative models. *arXiv preprint arXiv:1905.10887*, 2019.
- [60] R. M. Ryan and E. L. Deci. Intrinsic and extrinsic motivations: Classic definitions and new directions. *Contemporary educational psychology*, 25(1):54–67, 2000.
- [61] M. Savva, A. Kadian, O. Maksymets, Y. Zhao, E. Wijmans, B. Jain, J. Straub, J. Liu, V. Koltun, J. Malik, et al. Habitat: A platform for embodied ai research. In *Proceedings of the IEEE/CVF International Conference on Computer Vision*, pages 9339–9347, 2019.
- [62] M. Schwarzer, A. Anand, R. Goel, R. D. Hjelm, A. Courville, and P. Bachman. Data-efficient reinforcement learning with self-predictive representations. In *International Conference on Learning Representations*, 2021.
- [63] M. Schwarzer, N. Rajkumar, M. Noukhovitch, A. Anand, L. Charlin, D. Hjelm, P. Bachman, and A. Courville. Pretraining representations for data-efficient reinforcement learning. *arXiv preprint arXiv:2106.04799*, 2021.
- [64] A. W. Senior, R. Evans, J. Jumper, J. Kirkpatrick, L. Sifre, T. Green, C. Qin, A. Žídek, A. W. Nelson, A. Bridgland, et al. Improved protein structure prediction using potentials from deep learning. *Nature*, 577(7792):706–710, 2020.
- [65] P. Sermanet, C. Lynch, Y. Chebotar, J. Hsu, E. Jang, S. Schaal, S. Levine, and G. Brain. Time-contrastive networks: Self-supervised learning from video. In *2018 IEEE International Conference on Robotics and Automation (ICRA)*, pages 1134–1141. IEEE, 2018.
- [66] H. Singh, N. Misra, V. Hnizdo, A. Fedorowicz, and E. Demchuk. Nearest neighbor estimates of entropy. *American journal of mathematical and management sciences*, 23(3-4):301–321, 2003.
- [67] E. S. Spelke and K. D. Kinzler. Core knowledge. *Developmental science*, 10(1):89–96, 2007.
- [68] A. Stooke, K. Lee, P. Abbeel, and M. Laskin. Decoupling representation learning from reinforcement learning. In *International Conference on Machine Learning*, pages 9870–9879. PMLR, 2021.
- [69] R. S. Sutton and A. G. Barto. *Reinforcement learning: An introduction*. MIT press, 2018.
- [70] A. Szot, A. Clegg, E. Undersander, E. Wijmans, Y. Zhao, J. Turner, N. Maestre, M. Mukadam, D. S. Chaplot, O. Maksymets, et al. Habitat 2.0: Training home assistants to rearrange their habitat. *Advances in Neural Information Processing Systems*, 34, 2021.

- [71] J. Tack, S. Mo, J. Jeong, and J. Shin. Csi: Novelty detection via contrastive learning on distributionally shifted instances. *arXiv preprint arXiv:2007.08176*, 2020.
- [72] J. Tobin, W. Zaremba, and P. Abbeel. Domain randomization and generative models for robotic grasping. *CoRR*, abs/1710.06425, 2017.
- [73] H. van Hasselt, A. Guez, and D. Silver. Deep reinforcement learning with double q-learning. In *Proceedings of the Thirtieth AAAI Conference on Artificial Intelligence, February 12-17, 2016, Phoenix, Arizona, USA*, pages 2094–2100. AAAI Press, 2016.
- [74] R. D. Walk, J. D. Shepherd, and D. R. Miller. Attention and the depth perception of kittens. *Bulletin of the Psychonomic Society*, 26(3):248–251, 1988.
- [75] L. Weihs, A. Kembhavi, K. Ehsani, S. M. Pratt, W. Han, A. Herrasti, E. Kolve, D. Schwenk, R. Mottaghi, and A. Farhadi. Learning generalizable visual representations via interactive gameplay. *arXiv preprint arXiv:1912.08195*, 2019.
- [76] L. Wiskott and T. J. Sejnowski. Slow feature analysis: Unsupervised learning of invariances. *Neural computation*, 14(4):715–770, 2002.
- [77] Y. Wu, Y. Wu, G. Gkioxari, and Y. Tian. Building generalizable agents with a realistic and rich 3d environment. *arXiv preprint arXiv:1801.02209*, 2018.
- [78] D. Yarats, R. Fergus, A. Lazaric, and L. Pinto. Reinforcement learning with prototypical representations. *arXiv preprint arXiv:2102.11271*, 2021.
- [79] W. Ye, S. Liu, T. Kurutach, P. Abbeel, and Y. Gao. Mastering atari games with limited data. *Advances in Neural Information Processing Systems*, 34, 2021.
- [80] F. Yu, A. Seff, Y. Zhang, S. Song, T. Funkhouser, and J. Xiao. Lsun: Construction of a large-scale image dataset using deep learning with humans in the loop. *arXiv preprint arXiv:1506.03365*, 2015.

A Experiment Details on Representation Pretraining

We follow the same optimization step of SimSiam [11].

The input image size is 32×32 . We use SGD with base $lr = 0.03$ and a cosine decay [46] schedule for 800 epochs, weight decay = 0.0005, momentum = 0.9, and batch size = 512. The encoder f is a ResNet-18 [22] with the last fc layer removed.

We use the same projection and prediction networks in SimSiam. Specifically, the projection MLP g has 3 layers, and has BN applied to each fully-connected (fc) layer, including its output fc. There is no ReLU for the last fc layer in g and the hidden size is 2048. The prediction MLP (h) has 2 layers, and has BN applied to its hidden fc layers. Its output fc does not have BN or ReLU. The dimension of h 's input and output is $d = 2048$, and h 's hidden layer's dimension is 512, making h a bottleneck structure.

After pretraining, the representation encoder f is finetuned for downstream tasks.

B Representation Learning Loss and Pseudocode

We use the symmetrized cosine similarity loss from SimSiam. Specifically, for two consecutive observations s_1 and s_2 , denoting the two output vectors as $p_1 = h(g(f(s_1)))$ and $z_2 = g(f(s_2))$, we minimize their negative cosine similarity:

$$\mathcal{D}(p_1, z_2) = -\frac{p_1 \cdot z_2}{\|p_1\|_2 \cdot \|z_2\|_2}, \tag{1}$$

where $\|\cdot\|_2$ is ℓ_2 -norm. And the loss function is defined as

$$\begin{aligned} \mathcal{L} = & \frac{1}{2} \mathcal{D}(p_1, \text{stop_gradient}(z_2)) \\ & + \frac{1}{2} \mathcal{D}(p_2, \text{stop_gradient}(z_1)). \end{aligned} \tag{2}$$

Algorithm 1 shows the pseudocode of representation learning.

C Experiment and dataset details

Datasets CIFAR-10 [38] and CIFAR-100 [38] consist of 50,000 training and 10,000 test images with 10 and 20 (super-class) image classes, respectively. For CIFAR-10, out-of-distribution (OOD) samples are as follows: SVHN [49] consists of 26,032 test images with 10 digits, resized LSUN [80] consists of 10,000 test images of 10 different scenes, Interp. consists of 10,000 test images of linear interpolation of CIFAR-10 test images. CelebA [45], a labeled dataset consisting of over 200,000 face images and each with 40 attribute annotation. The Atari observation dataset is collected using double DQN [47, 73] with n-step return ($n=3$) and 3 frames stacking. In total we collected 50M images and each observation is resized to $64 \times 64 \times 3$.

Model details For CIFAR10, we use pretrained StyleGAN available at the official website of StyleGAN-Ada[31]². This pretrained model is a conditional StyleGAN that achieves best FID score. We also experimented with the model with best Inception score³ but did not observe significant difference in results.

For CIFAR100, since we did not find publicly available pretrained models, we trained one by ourself using the StyleGAN official code⁴.

²<https://nvlabs-fi-cdn.nvidia.com/stylegan2-ada-pytorch/pretrained/paper-fig11b-cifar10/cifar10c-cifar-ada-best-fid.pkl>

³<https://nvlabs-fi-cdn.nvidia.com/stylegan2-ada-pytorch/pretrained/paper-fig11b-cifar10/cifar10c-cifar-ada-best-is.pkl>

⁴<https://github.com/NVLabs/stylegan2-ada>

For Atari, we train an unconditional StyleGAN using the official code. It is difficult to train StyleGAN to converge on our Atari dataset with the default hyperparameters. We found that increasing the batch size to 256 significantly help stabilize the training and accelerate convergence.

Linear classification The quality of the pretrained representations is evaluated by training a supervised linear classifier on frozen representations h in the training set, and then testing it in the validation set. We use batch size of 512, Adam optimizer with learning rate being 0.001. We finetune for 100 epochs in linear classification experiments.

Atari games Our evaluation metric for an agent on a game is *human-normalized score* (HNS), defined as $\frac{agent_score - random_score}{human_score - random_score}$. We calculate this per game by averaging scores over 100 evaluation trajectories at the end of training, and across 10 random seeds for training. We report both mean (Mn) and median (Mdn) HNS over the 26 Atari-100K games, as well as on how many games a method achieves super-human performance ($>H$) and greater than random performance (>0).

D Experiment details on RL

We adhere closely to the parameter settings from URLB [41], which our implementation is based upon. We list the hyper-parameters in Table 4

We employ clipped double Q-learning for the critic, where each Q -function is parametrized as a 3-layer MLP with ReLU activations after each layer except of the last. The actor is also a 3-layer MLP with ReLUs that outputs mean and covariance for the diagonal Gaussian that represents the policy. The hidden dimension is set to 1024 for both the critic and actor. The actor and critic networks both have separate encoders, although we share the weights of the conv layers between them. Furthermore, only the critic optimizer is allowed to update these weights (e.g. we stop the gradients from the actor before they propagate to the shared conv layers).

Table 4: Hyper-parameters for training the unsupervised RL algorithms.

Random hyper-parameter	Value
Replay buffer capacity	10^6
Seed frames	4000
Mini-batch size	1024
Discount (γ)	0.99
Optimizer	Adam
Learning rate	10^{-4}
Agent update frequency	2
Critic target EMA rate	0.01
Hidden dim.	1024
Exploration stddev clip	0.3
Exploration stddev value	0.2
Reward transformation	$\log(r + 1.0)$
Forward net arch.	$(512 + \mathcal{A}) \rightarrow 1024 \rightarrow 512$ ReLU MLP
Inverse net arch.	$(2 \times 512) \rightarrow 1024 \rightarrow \mathcal{A} $ ReLU MLP
k in NN	12
Avg top k in NN	True
Episode length	200

Algorithm 1 Representation Learning Pseudocode

```
# f: backbone
# g: projection mlp
# h: prediction mlp

for x1, x2 in loader: # load tuples of consecutive observations
    h1, h2 = f(x1), f(x2) # representations, n-by-d
    z1, z2 = f(h1), f(h2) # projections, n-by-d
    p1, p2 = h(z1), h(z2) # predictions, n-by-d

    L = D(p1, z2)/2 + D(p2, z1)/2 # loss

    L.backward() # back-propagate
    update(f, h) # SGD update

def D(p, z): # negative cosine similarity
    z = z.detach() # stop gradient

    p = normalize(p, dim=1) # l2-normalize
    z = normalize(z, dim=1) # l2-normalize
    return -(p*z).sum(dim=1).mean()
```

Algorithm 2 Environment Pseudocode

```
# P: policy
# G: generator
# alpha, beta: hyperparameters control the importance of action and state.

for t in range(episode_length): #
    z = random_normal() # sample a random latent from Gaussian
    if t == 0: # first step of an episode
        z_t = z
        c = random_label() # sample a random class label
        s_t = G(z_t, c) # generate an observation
        a_t = P(s_t) # sample an action from policy
    else:
        zprime = alpha * a_t + (1 - alpha) * z
        z_t = beta * z_t + (1 - beta) * zprime
        s_t = G(z_t, c) # generate an observation
        a_t = P(s_t) # sample an action from policy
```
